Influence of Neutral Line to the Optimal Drive Current of PMAC Motors

Chao Bi, Nay Lin Htun Aung, Cheng Su Soh, Quan Jiang, Hla Nu Phyu, Yinqun Yu, and Song Lin

Data Storage Institute, A-STAR, 117608 Singapore

The optimal drive current can reduce both the torque ripple and power loss in driving the permanent magnetic (PM) AC motor. This paper presents an analytical model for calculating the optimal drive current of the PMAC motor with surface mount PM rotor. Both the motors with and without the neutral line are analyzed. Theoretical analysis shows that, when the back-emf of the windings contains triple order harmonics, the neutral line of the motor can let the optimal drive current be different from the one without the neutral line, and it can also make the optimal drive current be more effective in the loss and torque ripple reduction. Two spindle motors are used in the analysis to show the influences of the optimal model presented.

Index Terms—**Brushless motors, losses, optimal control, permanent magnet (PM) motors, torque control.**

I. Introduction

FROM the point of view of quantity, a permanent magnetic (PM) AC (PMAC) motor with surface mount PM rotor (SM-PMAC motor) is more popular than other types of PMAC motors. The spindle motor used in hard disk drive is the typical SM-PMAC motor, and the motor with nine slots and six magnetic pole-pair is shown in Fig. 1. For this kind of motor, in linear state, the winding inductance is independent of the rotor position; therefore its L_d and L_q are the same [1]. A concern is how to realize the optimal current in a SM-PMAC motor in many applications.

For the three-phase PMAC motors, a Y-connection is normally used, where the armature windings contain a neutral terminal. Whether the neutral terminal is linked to the drive system with a neutral line, or not, it depends on the drive mode used in the drive system. For some drive modes, the influence of the neutral line can be neglected, the motor system can thus be simplified to save the neutral line.

The optimal drive current is expected in the applications of all kinds of PMAC motors [2]–[18]. Here, the optimal drive current is defined as: the current which can generate the required electromagnetic (EM) torque with minimum copper loss and minimum torque ripple. It is clear, for the three-phase motor, the following nonlinear constraint optimization equation can be used for the definition and describing the ideal optimal drive current:

$$\begin{cases} \min_{[i_k]} \left\{ [i_k], \sum\limits_{k=a,b,c} i_k(\theta) \right\} \\ T_{\mathrm{em}}(i_a, i_b, i_c) = T_L \end{cases} \tag{1}$$

where T_{em} is the EM torque generated by the motor, and it is the function of the current in the three phase windings, i_a, i_b and i_c; T_L is the torque requested to drive the motor load.

The optimal drive current is expected, but what of the optimal currents for the motors with and without the neutral line? If they are different, what are the differences in the current waveform and what are their effects? Knowing the influence of the neutral line to the optimal drive current is necessary as it is important to realize a high performance PMAC motor system. In this paper, the analysis will be concentrated at the SM-PMAC motor. In the following analysis, SM-PMAC will be replaced by PMAC, unless noted otherwise.

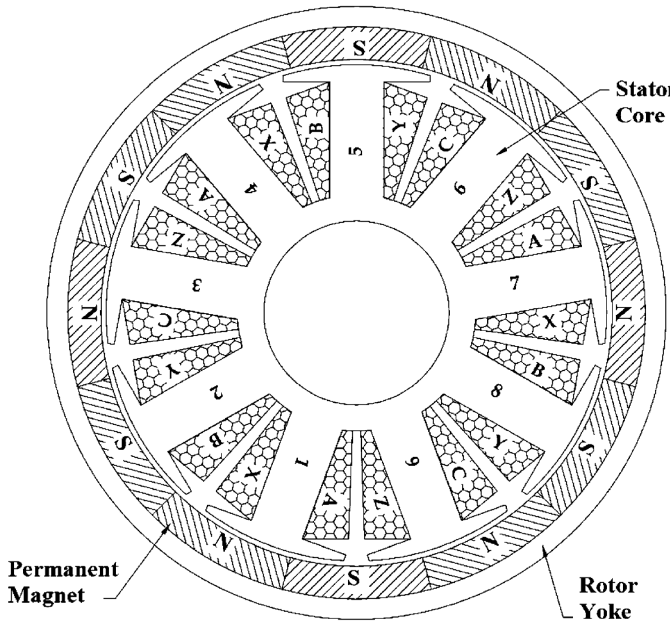

Fig. 1. Spindle motor with nine slots and six magnetic pole-pairs.

II. Model for Building Optimal Drive Current of PMAC Motor Without Neutral Line

The EM energy stored in a synchronous motor can be described as

$$\mathsf{E}_{co}(\theta) = \frac{1}{2}[i(\theta)]^T [L(\theta)][i(\theta)] \tag{2}$$

where [I] is the current in the motor windings, and $[L(\theta)]$ is the inductance of the windings. For the three-phase synchronous motor, its currents can be expressed as

$$[i]^T = [I_a(\theta), I_b(\theta), I_c(\theta), I_f] \tag{3}$$

Manuscript received November 26, 2012; revised February 03, 2013; accepted February 03, 2013. Date of current version May 30, 2013. Corresponding author: C. Bi (e-mail: BI_Chao@dsi.a-star.edu.sg).

Color versions of one or more of the figures in this paper are available online at http://ieeexplore.ieee.org.

Digital Object Identifier 10.1109/TMAG.2013.2245877

and the inductances can be expressed as

$$[L(\theta)] = \begin{bmatrix} L_a(\theta) & M_{ab}(\theta) & M_{ac}(\theta) & M_{af}(\theta) \\ M_{ba}(\theta) & L_b(\theta) & M_{bc}(\theta) & M_{bf}(\theta) \\ M_{ca}(\theta) & M_{cb}(\theta) & L_c(\theta) & M_{cf}(\theta) \\ M_{fa}(\theta) & M_{fb}(\theta) & M_{fc}(\theta) & L_f(\theta) \end{bmatrix}. \tag{4}$$

In (3), I_{f} is the rotor field current which generates the exciting magnetic field through rotor field winding, and it can be considered as a constant in the PMAC motor. In (4), L_i means the self-inductance of the ith winding, and M_{ij} means the mutual-inductance between the ith and jth phase windings. The subscript **f** means the ones related with the rotor winding.

The EM torque of the PMAC motor can be derived from its stored EM energy

$$T_{\mathrm{em}}(\theta) = \left.\frac{d\mathsf{E}_{co}(\theta)}{d\theta}\right|_{[i]=\mathrm{Const}} = \frac{1}{2}[i]^T\frac{d[L(\theta)]}{d\theta}[i]. \tag{5}$$

The $T_{\mathrm{em}}(\theta)$ can be further expressed as

$$T_{\mathrm{em}}(\theta) = T_A(\theta) + T_R(\theta) + T_{Cg}(\theta) \tag{6}$$

where

$$\begin{cases} T_A(\theta) = I_f\dfrac{d[M_f(\theta)]}{d\theta}[I] \\ T_R(\theta) = \dfrac{1}{2}[I]^T\dfrac{d[L_R(\theta)]}{d\theta}[I] + [I]^T\dfrac{d[M_S(\theta)]}{d\theta}[I] \\ T_{cg}(\theta) = \dfrac{1}{2}I_f^2\dfrac{dL_f(\theta)}{d\theta} \end{cases}. \tag{7}$$

In the previous equations, $T_A(\boldsymbol{\theta})$ is the alignment torque of the PMAC motor which is linearly proportional to the stator current $[I_s]$, and it is generated by the reaction between the stator field and rotor field. $T_R(\boldsymbol{\theta})$ is the reluctance torque induced by the reaction between the stator current $[i(\boldsymbol{\theta})]$ and the field produced by the stator current. $T_{cg}(\boldsymbol{\theta})$ is cogging torque caused by the reaction between the rotor field produced by I_f and the rotor equivalent current. For the PMAC motor in linear state, all the items in $[L(\theta)]$ are constant to the rotor position, except the ones related with the field winding, i.e., $[L(\theta)]$ can be rewritten as

$$[L(\theta)] = \begin{bmatrix} L_a & M_{ab} & M_{ac} & M_{af}(\theta) \\ M_{ba} & L_b & M_{bc} & M_{bf}(\theta) \\ M_{ca} & M_{cb} & L_c & M_{cf}(\theta) \\ M_{fa}(\theta) & M_{fb}(\theta) & M_{fc}(\theta) & L_f(\theta) \end{bmatrix}. \tag{8}$$

Therefore, in (6), the reluctance torque $T_R(\boldsymbol{\theta})$ is zero. For simplifying the analysis, the influence of the cogging torque $T_{cg}(\boldsymbol{\theta})$ in (6) is also neglected in the following analysis as they are normally very weak in the spindle motor. In this way, for a PMAC motor, its EM torque can be expressed as

$$\begin{aligned} T_{\mathrm{em}}(\theta) = T_A(\theta) &= I_f(\theta)\frac{d[M_f(\theta)]}{d\theta}[i(\theta)] \\ &= \frac{1}{\Omega}[e_a(\theta)\cdot i_a(\theta) + e_b(\theta) \\ &\quad \cdot i_b(\theta) + e_c(\theta)\cdot i_c(\theta)] \end{aligned} \tag{9}$$

where Ω is the motor speed, and $e_a(\theta)$, $e_b(\theta)$, and $e_c(\theta)$ are the back-emf of the A, B and C phase windings. In the following analysis, only the steady motor state is considered, i.e., the motor speed, Ω, is constant. Therefore, in the steady state, constant torque control means also constant power control.

When the neutral line of the armature winding is not used, the optimal current for the three-phase synchronous motor can be described with the following optimization equation with two constrained conditions:

$$\begin{cases} \min_{[i_k]}\left\{[i_k], \sum\limits_{k=a,b,c} i_k^2(\theta)\right\} \\ [e_a(\theta)\cdot i_a(\theta) + e_b(\theta)\cdot i_b(\theta) + e_c(\theta)\cdot i_c(\theta)]/\Omega = T_L \\ i_a(\theta) + i_b(\theta) + i_c(\theta) = 0 \end{cases} \tag{10}$$

or

$$\begin{cases} \min_{[i_k]}\left\{[i_k], \sum\limits_{k=a,b,c} i_k^2(\theta)\right\} \\ e_a(\theta)\cdot i_a(\theta) + e_b(\theta)\cdot i_b(\theta) + e_c(\theta)\cdot i_c(\theta) = P_L \\ i_a(\theta) + i_b(\theta) + i_c(\theta) = 0 \end{cases}. \tag{11}$$

In the previous equations, T_L is the EM torque requested, and $P_L = T_L\Omega$ is the EM power requested.

From the constrained conditions to the drive currents in (10), it can be known that

$$i_c = -(i_a + i_b). \tag{12}$$

The current model can thus be changed to

$$\begin{cases} \min_{[i_k]}\left\{[i_k], \sum\limits_{k=a,b} i_k^2(\theta) + I_a(\theta)I_b(\theta)\right\} \\ e_a(\theta)\cdot i_a(\theta) + e_b(\theta)\cdot i_b(\theta) - e_c(\theta)\cdot[i_a(\theta) + i_b(\theta)] = P_L \end{cases}. \tag{13}$$

As the magnet ring on the rotor is magnetized symmetrically, the back-emf of the windings are normally contains only the odd harmonics, and the examples used as follows will show that the high order harmonics decay rapidly with its order. Therefore, in the following analysis, only the fundamental, third-order and fifth-order harmonics in the back-emf will be considered in the analysis, that is

$$\begin{cases} e_a(\theta) = \sum\limits_{k=1}^{3} E_k\,\mathrm{Sin}[(2k-1)p\theta] \\ e_b(\theta) = \sum\limits_{k=1}^{3} E_k\,\mathrm{Sin}[(2k-1)p(\theta - 2\pi/3)] \\ e_c(\theta) = \sum\limits_{k=1}^{3} E_k\,\mathrm{Sin}[(2k-1)p(\theta - 4\pi/3)] \end{cases} \tag{14}$$

where p is the pole-pair of the motor.

Solving the first part of (13), the following equation can be obtained:

$$\begin{aligned} i_b = &\frac{-P_L - i_aE_1\left\{\mathrm{Cos}\left[p\left(\theta + \frac{\pi}{6}\right)\right] + \mathrm{Sin}(p\theta)\right\}}{\sqrt{3}E_1\,\mathrm{Cos}(p\theta) - E_5\,\mathrm{Cos}(5p\theta)\,\mathrm{Cos}(5p\pi/3)} \\ &+ \frac{i_aE_5\left\{\mathrm{Sin}(5p\theta) + \mathrm{Sin}\left[5p\left(\theta - \frac{4\pi}{3}\right)\right]\right\}}{\sqrt{3}E_1\,\mathrm{Cos}(p\theta) - E_5\,\mathrm{Cos}(5p\theta)\,\mathrm{Cos}(5p\pi/3)}. \end{aligned} \tag{15}$$

Using i_b in (15) to solve the second part of (13), it can generate

$$i_a = \frac{2P_L[E_1 \mathrm{Sin}(p\theta) + E_5 \,\mathrm{Sin}(5p\theta)]}{3\left[E_1^2 + E_5^2 - 2E_1E_5 \,\mathrm{Cos}(6p\theta)\right]}. \tag{16}$$

Using (12)–(16), it can be proven that for the three-phase motor without neutral line, its optimal current set, $\{i_{3l}\}$, is symmetric in space, that is

$$\begin{cases} i_{3l-a}(\theta) = \frac{2P_L[E_1 \,\mathrm{Sin}(p\theta) + E_5 \,\mathrm{Sin}(5p\theta)]}{3\left[E_1^2 + E_5^2 - 2E_1E_5 \,\mathrm{Cos}(6p\theta)\right]} \\ i_{3l-b}(\theta) = i_{3l-a}\left(\theta - \frac{2\pi}{3}\right) \\ i_{3l-c}(\theta) = i_{3l-a}\left(\theta - \frac{4\pi}{3}\right) \end{cases}. \tag{17}$$

From (17), it can be shown that for the three-phase PMAC motor without neutral line, its optimal drive current is not related with the third-order harmonic of the back-emf generated in the motor windings.

Let us consider a special case where the back-emf of the motor is sinusoidal, i.e.,

$$\begin{cases} e_a(\theta) = E_m \,\mathrm{Sin}(p\theta) \\ e_b(\theta) = E_m \,\mathrm{Sin}\left[p\left(\theta - \frac{2\pi}{3}\right)\right] \\ e_c(\theta) = E_m \,\mathrm{Sin}\left[p\left(\theta - \frac{4\pi}{3}\right)\right] \end{cases}. \tag{18}$$

From (17), the optimal drive current becomes

$$\begin{cases} i_{3l-a}(\theta) = \frac{2P_L}{3E_m} \,\mathrm{Sin}(p\theta) \\ i_{3l-b}(\theta) = \frac{2P_L}{3E_m} \,\mathrm{Sin}\left[p\left(\theta - \frac{2\pi}{3}\right)\right] \\ i_{3l-c}(\theta) = \frac{2P_L}{3E_m} \,\mathrm{Sin}\left[p\left(\theta - \frac{4\pi}{3}\right)\right] \end{cases}. \tag{19}$$

That is, the drive current is also sinusoidal. The result is quite meaningful as it confirms that if the high-order harmonics in the motor back-emf can be neglected, the sinusoidal current is reasonable to many PMAC motors.

III. Model for Building Optimal Drive Current of PMAC Motor With Neutral Line

When the neutral line is used, the last constraint condition in (10) disappears, therefore, the optimal drive current should be derived through the following:

$$\begin{cases} \min_{[i_k]} \left\{ [i_k], \sum_{k=a,b,c} i_k^2(\theta) \right\} \\ e_a(\theta)\cdot i_a(\theta) + e_b(\theta)\cdot i_b(\theta) + e_c(\theta)\cdot i_c(\theta) = P_L \end{cases}. \tag{20}$$

Consider the same back-emf described by (14), i.e., only the fundamental, third-order and fifth-order harmonics in the back-emf will be considered in the analysis. The first part of (20) can thus be used to eliminate $i_c(\theta)$, that is

$$i_c(\theta) = \frac{P_L + E_1 i_b \,\mathrm{Cos}\left(x - \frac{\pi}{6}\right) - E_1 i_a \,\mathrm{Sin}(\theta)}{E_1 \,\mathrm{Cos}\left(\theta + \frac{\pi}{6}\right) + E_3 \,\mathrm{Sin}(3\theta) + E_5 \,\mathrm{Sin}\left[5\left(\theta - \frac{4\pi}{3}\right)\right]} - \frac{E_3 \,\mathrm{Sin}(3\theta)(i_a + i_b) + E_5 i_a \,\mathrm{Sin}(5\theta) + E_5 i_b \,\mathrm{Sin}\left[5\left(\theta - \frac{2\pi}{3}\right)\right]}{E_1 \,\mathrm{Cos}\left(\theta + \frac{\pi}{6}\right) + E_3 \,\mathrm{Sin}(3\theta) + E_5 \,\mathrm{Sin}\left[5\left(\theta - \frac{4\pi}{3}\right)\right]}. \tag{21}$$

The second part of (20) can thus be used to generate the simultaneous equations in (22), shown at the bottom of the page, where

$$\begin{aligned} Z(\theta) = {} & P_L + E_1 i_b \,\mathrm{Cos}\left(\theta - \frac{\pi}{6}\right) - E_1 i_a \,\mathrm{Sin}(\theta) \\ & - E_3 \,\mathrm{Sin}(3\theta)(i_a + i_b) - E_5 i_a \,\mathrm{Sin}(5\theta) \\ & - E_5 i_b \,\mathrm{Sin}\left[5\left(\theta - \frac{2\pi}{3}\right)\right]. \end{aligned} \tag{23}$$

Solving (22), it can generate $\{i_{4l}\}$, the optimal drive current set for the three-phase PMAC motor with neutral line, and the set is symmetrical in space as:

$$\begin{cases} i_{4l-a}(\theta) = \frac{2P_L[E_1 \,\mathrm{Sin}(p\theta) + E_3 \,\mathrm{Sin}(3p\theta) + E_5 \,\mathrm{Sin}(5p\theta)]}{3\left[E_1^2 + E_3^2 + E_5^2 - (E_3^2 + 2E_1E_5)\,\mathrm{Cos}(6p\theta)\right]} \\ i_{4l-b}(\theta) = i_{4l-a}\left(\theta - \frac{2\pi}{3}\right) \\ i_{4l-c}(\theta) = i_{4l-a}\left(\theta - \frac{4\pi}{3}\right) \end{cases}. \tag{24}$$

Let us reconsider the special case where the back-emf of the motor is sinusoidal. In this case, from (24), the optimal drive current becomes

$$\begin{cases} i_{4l-a}(\theta) = \frac{2P_L}{3E_m} \,\mathrm{Sin}(p\theta) \\ i_{4l-b}(\theta) = \frac{2P_L}{3E_m} \,\mathrm{Sin}\left[p\left(\theta - \frac{2\pi}{3}\right)\right] \\ i_{4l-c}(\theta) = \frac{2P_L}{3E_m} \,\mathrm{Sin}\left[p\left(\theta - \frac{4\pi}{3}\right)\right] \end{cases}. \tag{25}$$

That is, the drive current is also sinusoidal in this case. Therefore, if the back-emf is purely sinusoidal one, the neutral line is not necessary to the optimal drive current. The result confirms again that the sinusoidal current is reasonable to many PMAC motors.

$$\begin{cases} i_a - \frac{[E_1 \,\mathrm{Sin}(\theta) + E_3 \,\mathrm{Sin}(3\theta) + E_5 \,\mathrm{Sin}(5x)]Z(\theta)}{\left\{E_1 \,\mathrm{Cos}\left(\theta + \frac{\pi}{6}\right) + E_3 \,\mathrm{Sin}(3\theta) + E_5 \,\mathrm{Sin}\left[5\left(\theta - \frac{4\pi}{3}\right)\right]\right\}^2} = 0 \\ i_b + \frac{\left\{E_1 \,\mathrm{Cos}\left(\theta - \frac{\pi}{6}\right) - E_3 \,\mathrm{Sin}(3\theta) - E_5 \,\mathrm{Sin}\left[5\left(\theta - \frac{2\pi}{3}\right)\right]\right\} Z(\theta)}{\left\{E_1 \,\mathrm{Cos}\left(\theta + \frac{\pi}{6}\right) + E_3 \,\mathrm{Sin}(3\theta) + E_5 \,\mathrm{Sin}\left[5\left(\theta - \frac{4\pi}{3}\right)\right]\right\}^2} = 0 \end{cases} \tag{22}$$

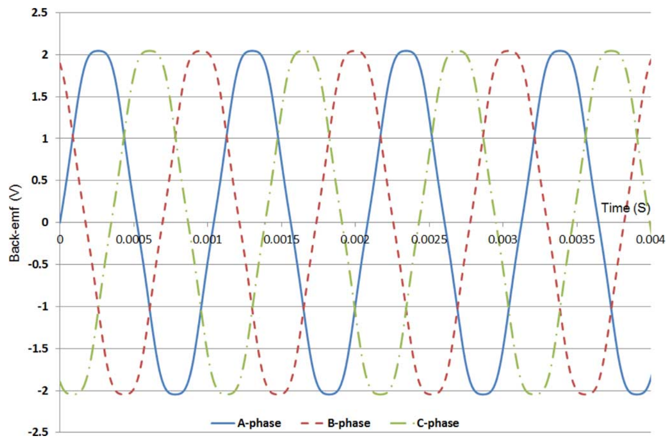

Fig. 2. M1: Three-phase back-emf.

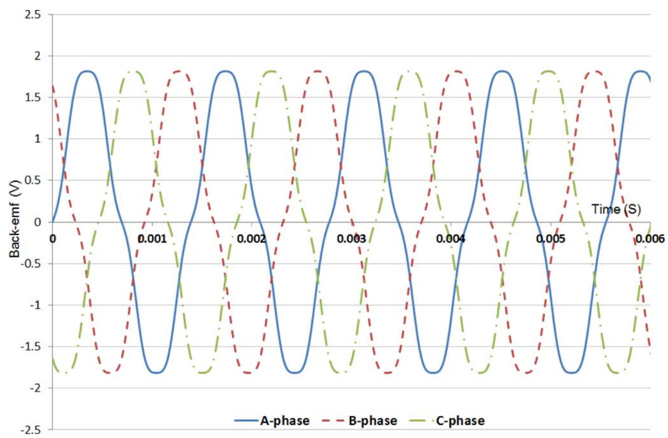

Fig. 3. M2: Three-phase back-emf.

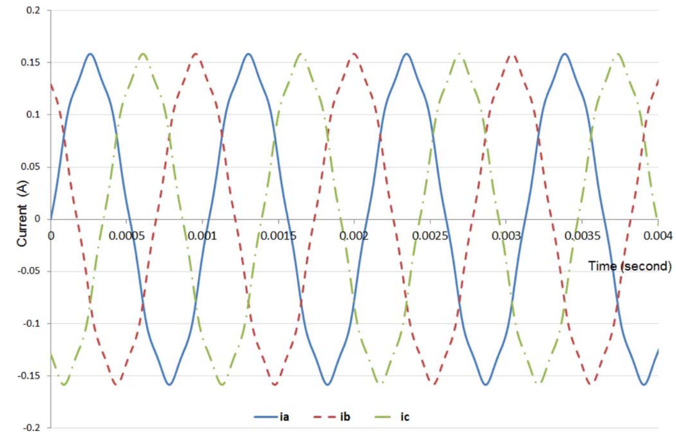

Fig. 4. M1: Optimal drive current.

TABLE I

M1: The amplitude of back-emf harmonics

Order	1	3	5	7	9
Amplitude (%)	100	0.313	3.204	0.169	0.086

TABLE II

M2: The amplitude of back-emf harmonics

Order	1	3	5	7	9
Amplitude (%)	100	-8.649	-6.486	0.267	0.0417

TABLE III

M1: The Relative Copper Losses of different drive modes

Drive mode	BLDC	Sinusoidal	Optimal
Copper loss	1	0.92237	**0.92246**

IV. Comparison of Optimal Drive Currents of the Two Connections

It was mentioned that, for the three-phase motor without natural line, the third harmonic of the back-emf cannot affect the optimal drive current of the motor; see (17). However, for the motor with natural line, (24) shows that the third harmonic of the back-emf can affect the optimal drive current. Anyway, these results show also that if the third order harmonic of the back-emf is zero, the expressions of $\{i_{3l}\}$ and $\{i_{4l}\}$ are same; i.e., the natural line has no meaning to the optimal drive current in the PMAC motor system. The results shown in (19) and (25) also confirm this phenomenon.

Comparing the expressions of $\{i_{3l}\}$ in (17) and $\{i_{4l}\}$ in (24), it can be found that they are quite similar. Their only difference is that $\{i_{4l}\}$ contains the components related with the third order harmonic of back-emf. It can be proven that if the back-emf contains third order harmonic, $\{i_{4l}\}$ is better than $\{i_{3l}\}$ in reducing the copper loss, and an example will be used to explain this phenomenon.

V. Analysis for Two Spindle Motors

It was mentioned that the spindle motor is a typical SM-PMAC motor. Two motors with this EM structure are used in the research, and they are called as M1 and M2 here. Figs. 2 and 3 shows the measured back-emfs of the motors. Both the motors are analyzed at 4200 r/min.

Tables I and II show the spectrum analysis results of the back-emf waveforms generated by M1 and M2, respectively. The tables show that, for the harmonic orders being higher than 7, their amplitudes are quite small and therefore can be neglected in the analysis. For M1, its third-order harmonic is also very weak. Therefore, according to the analysis in the Sections III and IV, the neutral line cannot affect its optimal drive current, i.e., only the current obtained without neutral line will be analyzed, and the simulated optimal current is shown in Fig. 4.

Using the optimal drive current (see Fig. 4) to drive M1, its simulated EM torque is shown both in Figs. 5 and 6. For comparison, the EM torques generated by the constant-current BLDC mode and "optimal sinusoidal current mode" are also shown in Figs. 5 and 6, respectively. The "optimal sinusoidal drive mode" can generate the sinusoidal drive current, and its phase angle is controlled in the way that the copper loss is the lowest in all the sinusoidal currents [18]. In using the different drive modes to drive M1, the currents were controlled in the way that the average torques generated by these drive modes are same. The figures show that, using the optimal current, the torque ripple can be eliminated. Though sinusoidal drive mode is better than constant-current BLDC mode, it still contains torque ripple.

For investigating the effect in the loss reduction with the optimal current, the copper losses of constant-current BLDC mode, "optimal sinusoidal drive mode" and optimal drive mode

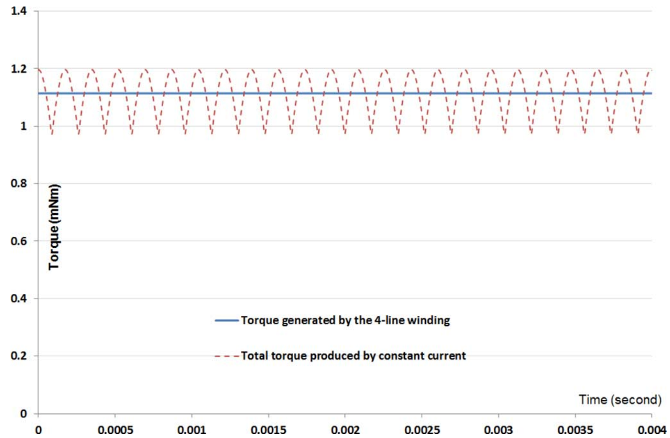

Fig. 5. M1: Torque generated by optimal drive current and BLDC current in constant-current mode.

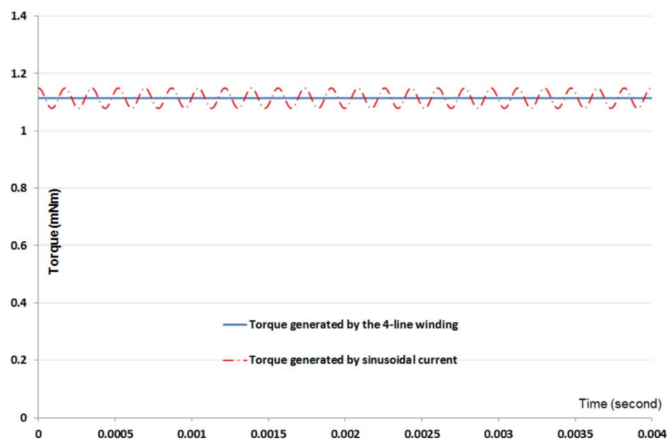

Fig. 6. M1: Torque generated by optimal and sinusoidal current.

are calculated for M1, and the simulated results are shown in Fig. 5. The EM torques generated by these drive modes are also shown in Fig. 5. In the table, for making the results clearer, the copper loss generated by the constant-BLDC mode is used as reference, and the loss values shown in the table are the ones comparing with the reference. From the table, sinusoidal is good in reducing the copper loss of M1.

As the back-emf waveform of M1 is quite close to sinusoidal, the copper loss of the optimal current is almost same as the one induced by sinusoidal drive mode. Anyway, the optimal current is derived by the condition that the torque ripple is zero, and the results shown in Fig. 6 confirm its effectiveness in the torque ripple reduction, which is better than sinusoidal current.

For M2, as its back-emf waveform contains third-order harmonic. Its optimal drive currents are different in the states with and without neutral line, and they are shown in Figs. 7 and 8, respectively.

EM torque of M2 generated by the optimal current is shown in Figs. 9 and 10. Both the torques generated by the optimal currents with and without neutral line are the same, and no torque ripple is induced by these optimal currents. For comparison, the EM torques generated by the constant-current BLDC mode is also shown in Fig. 9, and it contains rich torque ripple. The torque generated by "optimal sinusoidal current" is shown in

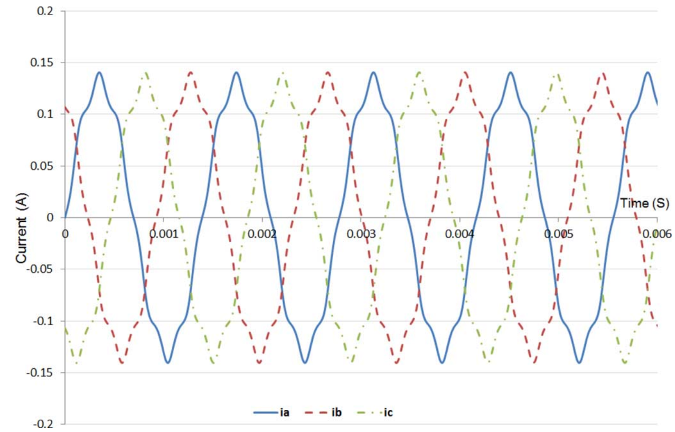

Fig. 7. M2: Optimal drive current without neutral line.

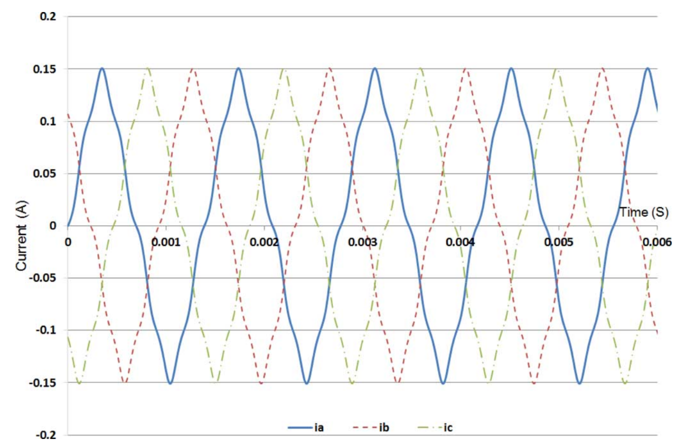

Fig. 8. M2: Optimal drive current with neutral line.

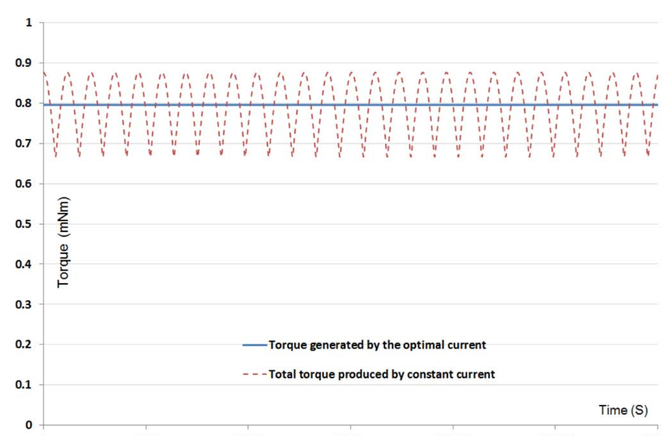

Fig. 9. M2: Torque generated by optimal drive current and BLDC current in constant-current mode.

Fig. 10, and it is clear that the current can also induce torque tipple in M2. It is same as the case in M1, in using the different drive modes to drive M2, the currents are controlled in the way that the average torques generated by these drive mode are the same. It can still be found that sinusoidal drive mode is better than constant-current BLDC mode in the torque ripple reduction, but it still contains torque ripple.

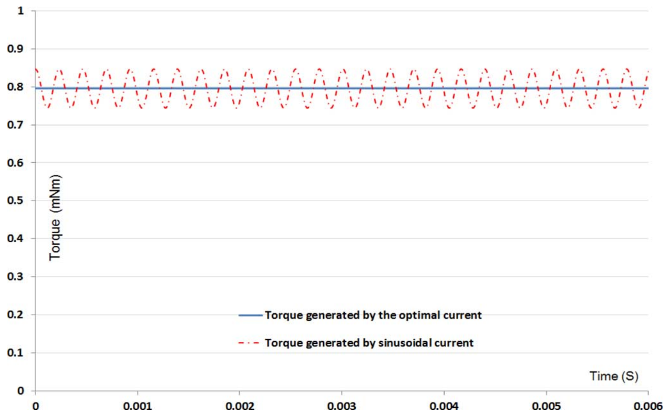

Fig. 10. M2: Torque generated by optimal current and sinusoidal current.

TABLE IV

M2: The Relative Copper Losses of different drive modes

Drive mode	BLDC	Sinusoidal	Optimal without neutral line	Optimal with neutral line
Copper loss	1	0.93419	0.93741	**0.92949**

Table IV shows the copper losses of the optimal current mode without and with natural line, sinusoidal current and constant-current BLDC mode in the operation of M2. The EM torque generated by these drive modes is shown in Fig. 9. In the table, the copper loss generated by the constant-BLDC drive mode is still used as reference. From the table, sinusoidal drive mode is still good in reducing the copper loss, but is still weaker than the optimal mode without neutral line. However, for M2, as its back-emf contains quite strong third-order harmonics, the best drive mode in the copper loss reduction is the optimal drive mode with neutral line.

VI. Conclusion

In this paper, the models for developing the optimal drive current of the three-phase motor with neutral and without neutral line are presented. From the current expressions deduced, the major difference between these two kinds of optimal drive currents is the influence of the third-order harmonics in the back-emf. For the three-phase motor without neutral line, the third harmonic of the back-emf cannot affect the current waveform. The simulation results on the two motors show that if the third-order harmonics of the motor is strong, the sinusoidal current cannot eliminate the EM torque ripple. However, both the optimal drive current with and without neutral line can eliminate the torque ripple efficiently. Besides, in torque ripple elimination, the optimal drive current with neutral line can even consume less copper loss than the sinusoidal current. However, in the examples used the difference in the copper losses of the optimal drive current with and without neutral lines are quite small. Therefore, the neutral line can be saved in the cases where the copper loss is not very concerned. The theoretical analysis results show that whether the neutral line is used or not, the optimal current can reduce the copper loss obviously and is better than the ones generated by BLDC constant current drive mode. Analysis shows that if the back-emf contains very weak harmonics, the optimal drive current is just the sinusoidal current, and the neutral line is not necessary in driving the motor.

References

[1] M. Štulrajter, V. Hrabovcová, and M. Franko, "Permanent magnet synchronous motor control theory," *J. Electrical Eng.*, vol. 58, no. 2, pp. 79–84, 2007.

[2] C. BI, N. P. Hla, C. S. Soh, and Q. Jiang, "An optimal drive current model and its application to reluctance motor," in *Proc. XIX Int. Conf. Electrical Machines (ICEM-2010)*, Rome, Italy, Sep. 6–8, 2010.

[3] N. V. Olarescu, M. Weinmann, S. Zeh, S. Musuroi, and C. Sorandaru, "Optimum current reference generation algorithm for PMSMS drive system for wide speed range," in *Proc. MELECON 2010–2010 15th IEEE Mediterranean Electrotechnical Conf.*, pp. 1073–1077.

[4] C. Mademlis, I. Kioskeridis, and N. Margaris, "Optimal efficiency control strategy for interior permanent magnet synchronous motor drives," *IEEE Trans. Energy Conversion*, vol. 19, no. 4, pp. 715–723, Dec. 2004.

[5] S. Shinnaka and T. Sagawa, "New optimal current control methods for energy-efficient and wide speed-range operation of hybrid-field synchronous motor," *IEEE Trans. Indust. Electron.*, vol. 54, no. 5, pp. 2443–2450, Oct. 2007.

[6] P. L. Chapman, S. D. Sudhoff, and C. A. Whitcomb, "Optimal current control strategies for surface-mounted PM synchronous machine drives," *IEEE Trans. Energy Conversion*, vol. 14, no. 4, pp. 1043–1050, Dec. 1999.

[7] K. Malekian, M. R. Sharif, and J. Milimonfared, "An optimal current vector control for synchronous reluctance motors incorporating field weakening," in *Proc. 10th IEEE Int. Workshop Advanced Motion Control*, Mar. 26–28, 2008, pp. 393–398, Issue.

[8] N. Bianchi, S. Bolognani, and M. Zigliotto, "Time optimal current control for PMSM drives," in *Proc. IECON 02*, Nov. 1, 2002.

[9] C. Mademlis and N. Margaris, "Loss minimization in vector-controlled interior permanent-magnet synchronous motor drives," *IEEE Trans. Indust. Electron.*, vol. 49, no. 6, pp. 1344–1347, Dec. 2002.

[10] Y. Nakamura, "High-efficiency drive due to power factor control of a permanent magnet synchronous motor," *IEEE Trans. Power Electron.*, vol. 10, no. 2, pp. 247–253, Mar. 1995.

[11] P. L. Chapman, S. D. Sudhoff, and C. A. Whitcomb, "Torque ripple minimization in permanent magnet synchronous servo drive," *IEEE Trans. Energy Conversion*, vol. 14, no. 3, pp. 616–621, Sep. 1999.

[12] C. Mademlis, J. Xypteras, and N. Margaris, "Loss minimization in surface permanent-magnet synchronous motor drives," *IEEE Trans. Indust. Electron.*, vol. 47, no. 1, pp. 115–122, Feb. 2000.

[13] C. Bi, Q. Jiang, S. Lin, T. S. Low, and A. A. Mamun, "Reduction of acoustic noise in FDB spindle motors by using drive technology," *IEEE Trans. Magn.*, vol. 39, pp. 800–805, Mar. 2003.

[14] S. Morimoto, Y. Takeda, and T. Hirasa, "Loss minimization control of permanent magnet synchronous motor drives," *IEEE Trans. Indust. Electron.*, vol. 41, no. 5, pp. 511–517, Oct. 1994.

[15] X. Ojeda, X. Mininger, M. Gabsi, and M. Lecrivain, "Sinusoidal feeding for switched reluctance machine: Application to vibration damping," in *Proc. Int. Conf. Electrical Machine, ICEM*, Vilamoura, Portugal, Sep. 6–9, 2008.

[16] T. S. Low, B. Chao, and K. T. Chang, "Motor identity'—A motor model for torque analysis and control," *IEEE Trans. Indust. Electron.*, vol. 43, no. 2, pp. 285–291, Apr. 1996.

[17] F. F. Bernal, A. García-Gerrada, and R. Faure, "Model-based loss minimization for DC and AC vector-controlled motors including core saturation," *IEEE Trans. Industry Applicat.*, vol. 36, no. 3, pp. 755–763, May/Jun. 2000.

[18] T. S. Low, B. Chao, and K. T. Chang, "Motor identity'—A motor model for torque analysis and control," *IEEE Trans. Indust. Electron.*, vol. 43, no. 2, pp. 285–291, Apr. 1996.